ACS Photonics

Letter

Cite This: ACS Photonics XXXX, XXX, XXX−XXX

pubs.acs.org/journal/apchd5

Single Fluorescent Peptide Nanodots

Nadezda Lapshina,*[,†] Jonathan Jeffet,[‡] Gil Rosenman,[†] Yuval Ebenstein,[‡,§] and Tal Ellenbogen[†,§]

[†]School of Electrical Engineering, Faculty of Engineering, [‡]School of Chemistry, Raymond and Beverly Sackler Faculty of Exact Sciences, and [§]Center for Light Matter Interaction, Tel-Aviv University, Ramat Aviv, 69978 Tel Aviv, Israel

Supporting Information

ABSTRACT: Fluorescent peptide nanodots (PNDs) are bioorganic nanoparticles self-assembled from peptide biomolecules of different origin and complexity. These recently discovered nanodots of biological origin are highly promising for biomedical imaging applications due to their biocompatibility, bright and tunable fluorescence over the entire visible range and photostability. Here we apply single-particle microscopy methods to study the photophysical properties of individual PNDs. We show that the fluorescence spectrum tunability, studied previously only for PND ensembles in solutions, origins at the single-particle level. Temporal dynamics measurements of the single particles reveal fluorescence lifetime in the range of nanoseconds and pronounced fluorescence blinking with continuous bright states of seconds. The latter provides a first evidence of quantum emitter transitions between two states (ON and OFF) in fluorescent PNDs. All these findings advance the understanding of the fluorescence mechanism of PNDs and provide strong motivation for using PNDs as fluorescent agents for various bioimaging and super-resolution techniques.

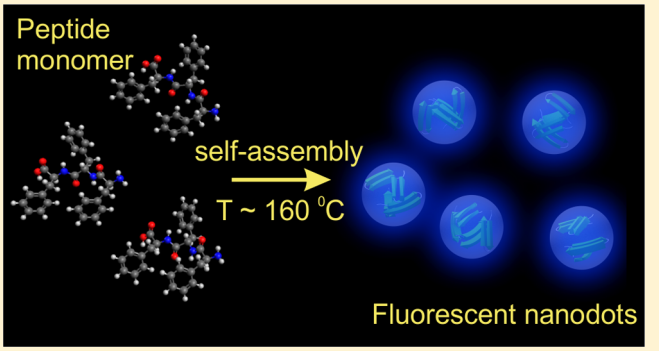

KEYWORDS: *peptide nanodots, fluorescence, single particle spectroscopy, lifetime, blinking, bioimaging*

Nanoscale fluorescence (FL) imaging is an essential tool for emerging biological and medical research and applications, for example, in precision medicine, where light diagnostics and therapy are applied at the level of a single diseased cell.[1] The capabilities of nanoscale FL imaging techniques are highly dependent on the used FL markers. Therefore, there is major interest in the development of novel FL agents. FL labels of different origins such as organic molecular dyes,[2] fluorescent proteins,[3,4] inorganic semiconductor quantum dots,[5,6] and carbon nanodots[7−9] were developed. They are distinct in their chemical and physical properties but should share common required figures of merit where biocompatibility and biodegradability are combined with high quantum yield, photostability, and nanoscale dimensions, in order, for example, to be incorporated into a single biocell and to be monitored by super-resolution microscopy techniques.

Recently, a new generation of bioinspired, inherently biocompatible, fluorescent peptide nanodots (PNDs) were discovered.[10] These bio-organic nanoparticles, composed from a variety of synthetic short peptides, exhibit bright and tunable visible FL. It was demonstrated that the self-assembled PNDs do not possess any visible FL in their initial state. However, they become FL under thermally mediated refolding of their biological secondary structure from original metastable α-helical to stable β-sheet structure.[10−12] This visible FL effect, found in ultrashort di- and tripeptide nanostructures and PNDs,[10−12] has similar physical origin as the FL effect revealed in amyloid fibrils,[13,14] nonaromatic biogenic and synthetic peptides,[15] native silk fibrils[16] and in recently developed new synthetic PEGylated peptide (PEG-hexaphenylalanine) and its derivatives.[17,18] This suggests that various types of originally nonfluorescent peptide (or even protein) nanodots and nanostructures can be converted into multicolor visible FL bionanoparticles, regardless of their original biomolecular composition. The physical origin of this new biophotonic fluorescent effect is completely different from inorganic counterpart quantum dots, carbon dots and organic dyes. One leading explanation for the FL mechanism in PNDs and other β-sheet rich nanostructures is ascribed to the strong hydrogen bonds which stabilize the supramolecular refolded β-sheets structure. As was shown by quantum molecular modeling,[13,14,19,20] these bonds allow proton transfer across the bond when excited to the first or higher energetic states. This proton transfer results in a modified molecular energy spectrum corresponding to red-shifted emission tunable over the whole visible range via variations in the excitation energy. Recent experiments with ensembles of PNDs[10] fully confirmed this picture.

The main attractive features of these recently discovered fluorescent PNDs, with respect to existing fluorescent agents, are their small size of several nanometers, biocompatibility, photostability, and relatively high quantum yield of ∼30%,[10]

Received: May 10, 2019
Published: June 7, 2019

DOI: 10.1021/acsphotonics.9b00685
ACS Photonics XXXX, XXX, XXX−XXX

which is in the typical range that is applicable for bioimaging studies,[21] and broadly tunable fluorescence within the wavelengths range of 420−650 nm. The latter property, which is absent in conventional dyes and inorganic quantum dots, allows to use a broad range of lasers as an excitation source. Finally, PNDs are also cheap and simple to synthesize. Even though existing biomarkers possess some of the properties above, it is hard to find a single biolabel with all these features. All together, these special features make PNDs highly promising for a wide variety of potential applications in high-resolution fluorescence bioimaging and advanced light-induced precision medical trials,[1] such as optical biopsy[22] and optogenetics.[23]

Up to date, studies of FL effects of PNDs were conducted on PND ensembles immersed in organic solution.[10] In this case, the measured FL signal is averaged over all emitters and can be affected, for example, by particles nonuniformities, particles interactions, and their environment. Therefore, investigation at a single-particle level is essential in order to characterize the photophysical properties of single PNDs and their applicability as new fluorescent labels.

Here, we applied single-molecule microscopy methods to characterize the optical properties of discrete PNDs self-assembled from aromatic triphenylalanine (FFF) peptide biomolecules. Our extensive studies included single PND FL imaging, spectral characterization of the emission, FL lifetime and emission intermittency measurements. These studies revealed, that the fluorescent spectrum tunability of PNDs that was measured for PND ensembles in solution[10] originates at the single-particle level. Moreover, it was found that the FL spectra of single particles are narrowed, and their peak location varies over ∼30 nm with respect to ensemble spectrum and peak location. Lifetime measurements reveal a biexponential decay with a mean value of ∼1.27 ns. Finally, we found pronounced intermittency in the emission intensity and observed continual bright states with a duration in the range of seconds. These observations represent for the first time the quantum emitter nature of PNDs.

Self-assembled PNDs were prepared by the use of "bottom-up" approach. At the beginning, a solution of native FFF-PNDs was prepared by the following procedure: the lyophilized powder of FFF (Bachem, Switzerland) was dissolved in 1,1,1,3,3,3-hexafluoro-2-propanol (HFIP; Sigma-Aldrich) to an initial concentration of 100 mg/mL, mixed in a vortex mixer (VELP Scientifica), and further diluted to a final concentration of 1 mg/mL in ethylene glycol (EG; Sigma-Aldrich). At this stage, FFF biomolecules nucleate into nanoscale seeds of a critical size representing FFF-PNDs.[24,25] The preceding self-organization process into larger nano- and microstructures was inhibited by adding EG.[10] This resulted in a solution containing PNDs. At this preliminary stage, the PNDs do not demonstrate any visible fluorescence. In order to prepare fluorescent PNDs, the native PND solution in EG was heated slowly from room temperature up to 160 °C and fixed at this temperature for 3 h. Then the solution was cooled down back to room temperature. EG was chosen as a solvent because of its high boiling point of 195 °C. By applying such a thermal treatment to the PND-EG, the nanodots' peptide secondary structure is transformed from an original α-helical structure to a β-sheet-rich structure.[10−12] As was shown in ref 10, this structural transition of the PNDs is accompanied by the onset of visible FL phenomenon. The formation process of visible PNDs is illustrated in Figure 1.

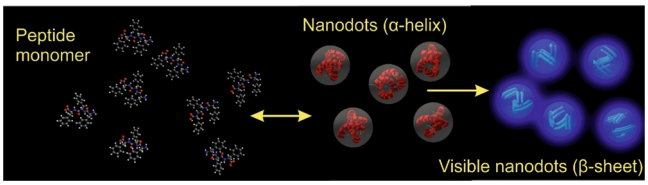

Figure 1. Formation process of visible PNDs. At the first stage, due to molecular recognition, individual peptide molecules are self-organized into nanodots having an α-helix peptide secondary structure. At the next stage, these nanodots are subjected to thermal treatment up to 160 °C for 3 h in order to refold the original biomolecular organization from an α-helix to a β-sheet secondary structure. Such refolding leads to the onset of the unique tunable visible fluorescent properties of PNDs.

For the preparation of dry samples with individual nanodots, a solution of FFF-PNDs in spectroscopic grade EG (initial concentration is 1 mg/mL) was diluted to 1:1000 in acetone. A drop of this solution was put on a precleaned quartz microscope slide and immediately covered by a precleaned coverslip in order to immobilize the PNDs and to prevent dust and residue contamination. The detailed cleaning procedure is described in the Supporting Information.

First, we imaged the individual PNDs with a single-molecule fluorescence microscope (ONI Nanoimager S) equipped with four continuous wave (CW) lasers operating at 375, 473, 532, and 640 nm. Figure 2a represents an absorption curve of the FFF-PND ensemble in EG solution with corresponding excitation wavelengths marked by arrows. Figure 2b shows epi-fluorescence images of individual PNDs dispersed on the coverslip and excited by the four different lasers. It can be clearly seen that the same nine single nanoparticles are fluorescent under 473 and 532 nm excitations. Particle numbers 1, 3, 5, and 9 also emit light under 375 nm excitation and there is no light emission for 640 nm excitation, as expected from the optical absorption graph (Figure 2a). The lack of the signal observed under 375 nm excitation for some of the dots may be attributed to the low excitation power we had at 375 nm (60 mW at 375 nm vs 600 mW at three other wavelengths). In addition, the FL signal is noisier due to possible residual FL in the optical path excited by the UV light.

To characterize the FL spectra of the individual visible PNDs, we constructed an experimental setup based on an inverted optical microscope coupled to a tunable pulsed excitation source, imaging spectrometer and lifetime measurement system as depicted in Figure 3(a) and also detailed in the Supporting Information.

First, we used the system to measure the FL from an ensemble of FFF-PNDs in EG solution. Emitted light was directed to an imaging spectrometer (Andor Shamrock 303) coupled to an EMCCD camera (Newton 970), and the emission spectra were acquired for different excitation wavelengths. Figure 3b shows the emission spectra for excitation laser tuned to 420, 502, and 525 nm. The measurements agree well with previously reported emission spectra.[10]

Then using the same experimental setup we measured the spectral characteristics for individual PNDs. In these studies we utilized the same sample as was used for epi-fluorescence imaging mentioned in previous section. Figure 4a−c shows fluorescent images of three isolated PNDs and their emission spectra obtained under 420 nm (425 nm dichroic mirror, 430 nm long pass emission filter), 502 nm (532 nm dichroic

DOI: 10.1021/acsphotonics.9b00685
ACS Photonics XXXX, XXX, XXX−XXX

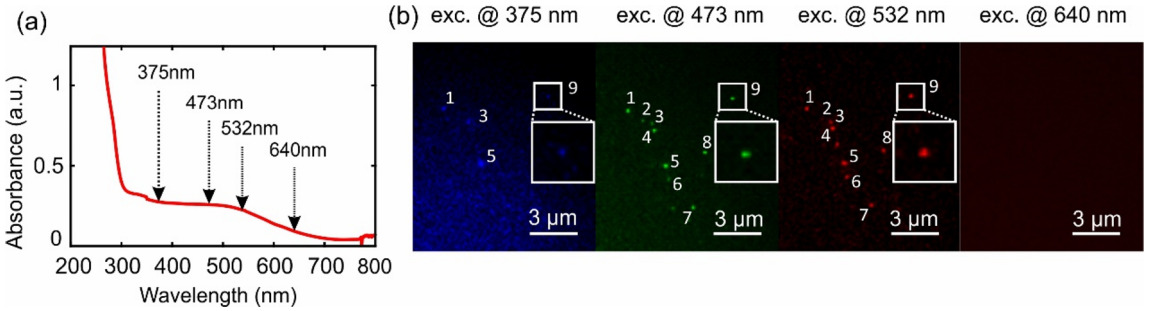

Figure 2. (a) Optical absorption curve of FFF PNDs in EG solution with applied excitation wavelengths marked by arrows. (b) Fluorescence images of the same single peptide dots excited at 375, 473, 532, and 640 nm (inserts show the same individual dot # 9 excited at different wavelengths). Each visible nanodot is indicated by a number. The last image shows that no fluorescence is measured under 640 nm excitation, which is consistent with the absorbance curve.

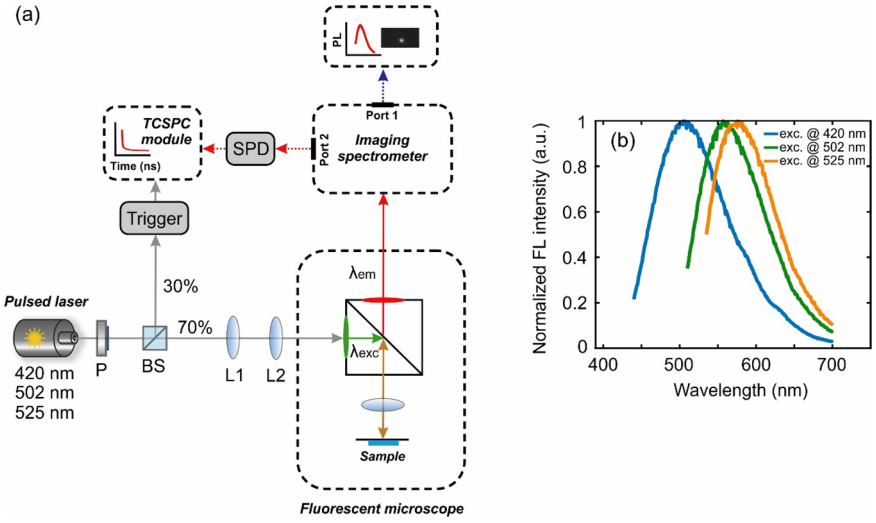

Figure 3. (a) Experimental setup for optical characterization of single PNDs. P, polarizer; BS, beam splitter; L, lens; SPD, single photon detector; TCSPC module, time-correlated single photon counting module. (b) Fluorescence spectra of FFF-PND ensemble in EG solution under three excitations (420, 502, and 525 nm).

mirror, 550 nm long pass emission filter), and 525 nm (532 nm dichroic mirror, 550 nm long pass emission filter) excitation wavelengths. It is important to note that the fluorescence spectra of the single PNDs and its tunability coincides with the spectra and tunability measured for PND ensembles in EG solution (Figure 1c). This provides strong evidence that the tunability of PND fluorescence is a property of the individual PNDs and is not a result of an inhomogeneous mixture of different emitters. However, a closer look (see Figure 4d) shows that the single nanoparticle fluorescence spectra are narrower than the ensemble spectra and that the emission maxima of different PNDs varies over ~30 nm. Thus, under 420 nm excitation a full width at half-maximum (fwhm) is ~65 nm for individual dots versus ~115 nm for the ensemble. Whereas when excited at 525 nm fwhm is ~90 nm for individual dots versus ~100 nm for the ensemble. Such an effect of spectral wandering is common for different types of single emitters such as molecular dyes,[26] carbon dots,[27] and quantum dots,[28] and can be attributed to changes of local molecule/particle nanoenvironments.[29]

In addition, we measured the temporal dynamics of the fluorescence for short and long time scales. First, we used femtosecond excitation and TCSPC system to measure fluorescence lifetimes of the individual PNDs (λ_{exc} = 502 nm, λ_{em} = 550 nm). Fluorescence decay of one representative PND approximated with biexponential fit is shown in Figure 5a (additional typical decays of other PNDs can be found in the Supporting Information, Figure S1). Calculated mean lifetime of individual PNDs is ~1.27 ± 0.12 ns. This is shorter compared to previous measurements of PNDs ensembles in solution that showed, for instance, a mean lifetime of ~3.6 ns for 550 nm excitation.[10] This difference can be attributed to the different local environment of the PNDs in the two experiments. It should be noted that the obtained lifetime value is at the same range as organic dyes which are commonly used as optical markers and also as optical gain material in laser technology.[30]

In the longer time scales, a unique effect, found in many types of single emitters, is an intermittency in emission intensity, or so-called fluorescence blinking. This effect results in fluctuation of the fluorescence intensity between bright (ON) and dark (OFF) states under constant laser illumination.[31] Blinking with discrete OFF-states from several milliseconds to hours was shown for different quantum emitters, such as inorganic quantum dots,[32−34] carbon dots,[35,36] fluorescent proteins, and organic dyes.[37] To examine blinking effects of PNDs we measured fluorescence time traces at room temperature using CW laser excitation. Pronounced blinking effects were observed. Figure 5b shows an example of individual PND fluorescence intensity fluctuations obtained

DOI: 10.1021/acsphotonics.9b00685
ACS Photonics XXXX, XXX, XXX−XXX

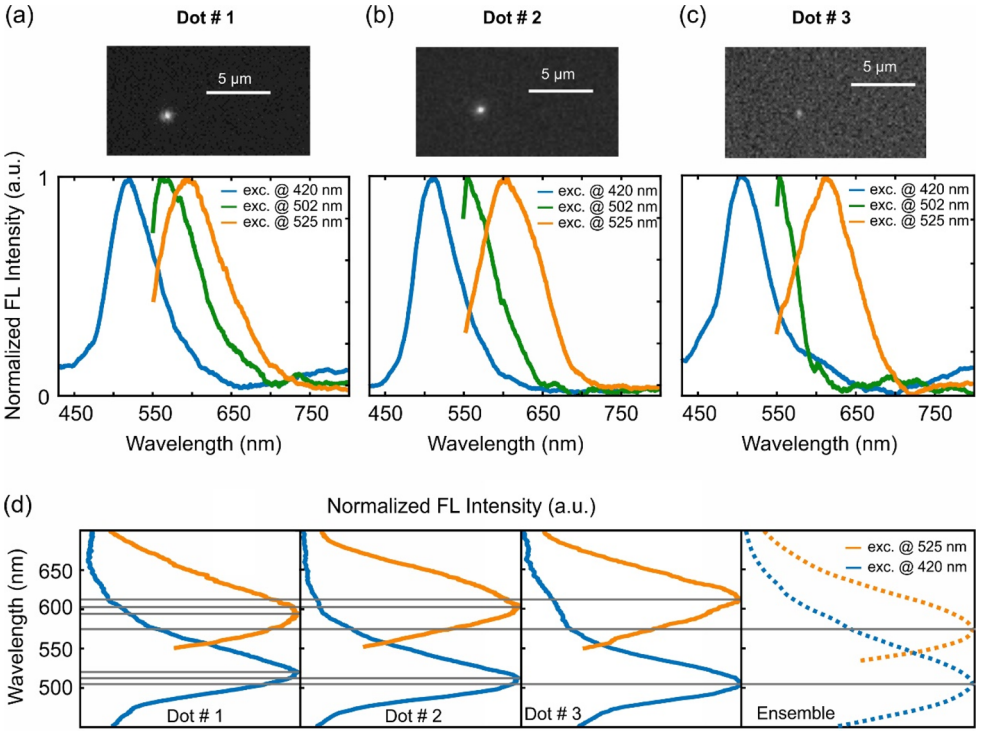

Figure 4. (a–c) Upper panels show fluorescence images of three individual peptide dots excited at 502 nm, lower panels represent emission spectra of each single dot excited at 420, 502, and 525 nm. (d) Fluorescence spectra of three single PNDs dispersed on a quartz microscope slide compared to that of PND ensemble suspended in EG.

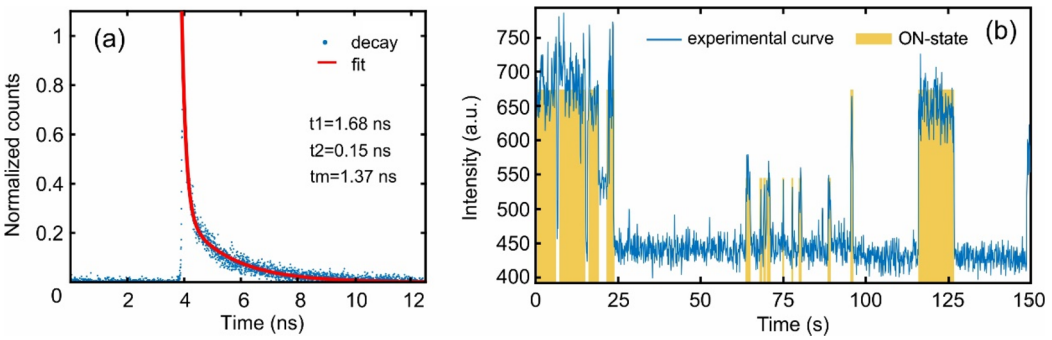

Figure 5. (a) Fluorescence lifetime of isolated PND taken at λ_{exc} = 502 nm. Fluorescence decay is fitted with a superposition of two exponential functions. (b) Long scale time trace of fluorescence intensity of an individual PND excited by CW laser (λ_{exc} = 532 nm). The blue curve shows the experimental data, the yellow areas represent ON-states of the PND emission.

at λ_{exc} = 532 nm, laser power density of 37.5 kW/cm^2, and measured with 10 Hz frame rate (more graphs of other PNDs can be found in the Supporting Information, Figure S2). It can be seen that the PND fluorescence turns ON and OFF with a time scale in the range of seconds. Such blinking characteristics with pronounced single-step transitions to ON/OFF-state can be attributed to a single quantum emitter behavior.[36] This observation opens the door to a plethora of applications and additional quantum emitter studies of PNDs.

To conclude, we performed extensive optical characterizations of single PND emitters. We found that the fluorescence spectrum tunability measured for PND ensembles origins at single-particle level accompanied by an effect of slight spectral dispersion for different individual particles. This wide spectral tunability, at the single particle level, may mark PNDs as promising candidates for broadband nanoscale light sources. Fluorescence lifetime studies demonstrated short time scales decay with a typical value of ~1.27 ± 0.12 ns. Along with their relatively high quantum yield, this may indicate their suitability as new biocompatible fluorescent probes as well as optical gain material. Long time scale measurements revealed pronounced fluorescence blinking involving continuous bright states with a duration in the range of seconds. This gives first evidence of the quantum emitter nature of fluorescent PNDs. It therefore opens the door to additional quantum emitter experiments with PNDs. Moreover, it marks PNDs as attractive for various blinking based super-resolution techniques, such as stochastic optical reconstruction microscopy (STORM).[38]

■ ASSOCIATED CONTENT

Supporting Information

The Supporting Information is available free of charge on the ACS Publications website at DOI: 10.1021/acsphotonics.9b00685.

DOI: 10.1021/acsphotonics.9b00685
ACS Photonics XXXX, XXX, XXX–XXX

Cleaning protocol of substrates, experimental setup for optical characterization of individual PNDs, and additional graphs of lifetime decays and blinking (PDF)

AUTHOR INFORMATION

Corresponding Author

*E-mail: lapshina.nadezda@gmail.com.

ORCID

Nadezda Lapshina: 0000-0002-8957-0549

Gil Rosenman: 0000-0002-0407-6163

Yuval Ebenstein: 0000-0002-7107-7529

Notes

The authors declare no competing financial interest.

ACKNOWLEDGMENTS

This project was supported by the Ministry of Science, Technology and Space of Israel. The authors thank Dr. Roman Noskov for insights and comments. J.J. is grateful to the Azrieli Foundation for the award of an Azrieli Fellowship.

REFERENCES

(1) Yun, S. H.; Kwok, S. J. J. Light in Diagnosis, Therapy and Surgery. *Nat. Biomed. Eng.* **2017**, *1*, 1−16.

(2) Schnermann, M. J. Organic Dyes for Deep Bioimaging. *Nature* **2017**, *551*, 176−177.

(3) Chudakov, D. M.; Matz, M. V.; Lukyanov, S.; Lukyanov, K. A. Fluorescent Proteins and Their Applications in Imaging Living Cells and Tissues. *Physiol. Rev.* **2010**, *90*, 1103−1163.

(4) Shaner, N. C.; Steinbach, P. A.; Tsien, R. Y. A Guide to Choosing Fluorescent Proteins. *Nat. Methods* **2005**, *2*, 905−909.

(5) Alivisatos, A. P. Semiconductor Clusters, Nanocrystals, and Quantum Dots. *Science* **1996**, *271*, 933−937.

(6) Michalet, X.; Pinaud, F.; Lacoste, T. D.; Dahan, M.; Bruchez, M. P.; Alivisatos, A. P.; Weiss, S. Properties of Fluorescent Semiconductor Nanocrystals and Their Application to Biological Labeling. *Single Mol.* **2001**, *2*, 261−276.

(7) Hola, K.; Zhang, Y.; Wang, Y.; Giannelis, E. P.; Zboril, R.; Rogach, A. L. Carbon Dots - Emerging Light Emitters for Bioimaging, Cancer Therapy and Optoelectronics. *Nano Today* **2014**, *9*, 590−603.

(8) Zhang, J.; Yu, S. H. Carbon Dots: Large-Scale Synthesis, Sensing and Bioimaging. *Mater. Today* **2016**, *19*, 382−393.

(9) Mintz, K. J.; Zhou, Y.; Leblanc, R. M. Recent Development of Carbon Quantum Dots Regarding Their Optical Properties, Photoluminescence Mechanism, and Core Structure. *Nanoscale* **2019**, *11*, 4634−4652.

(10) Lapshina, N.; Shishkin, I. I.; Nandi, R.; Noskov, R. E.; Barhom, H.; Joseph, S.; Apter, B.; Ellenbogen, T.; Natan, A.; Ginzburg, P.; Amdursky, N.; Rosenman, G. Bioinspired Amyloid Nanodots with Visible Fluorescence. *Adv. Opt. Mater.* **2019**, *7*, 1801400.

(11) Handelman, A.; Kuritz, N.; Natan, A.; Rosenman, G. Reconstructive Phase Transition in Ultrashort Peptide Nanostructures and Induced Visible Photoluminescence. *Langmuir* **2016**, *32*, 2847−2862.

(12) Handelman, A.; Lapshina, N.; Apter, B.; Rosenman, G. Peptide Integrated Optics. *Adv. Mater.* **2018**, *30*, 1705776.

(13) Chan, F. T. S.; Kaminski Schierle, G. S.; Kumita, J. R.; Bertoncini, C. W.; Dobson, C. M.; Kaminski, C. F. Protein Amyloids Develop an Intrinsic Fluorescence Signature during Aggregation. *Analyst* **2013**, *138*, 2156−2162.

(14) Kaminski, C. F.; Kaminski Schierle, G. S. Probing Amyloid Protein Aggregation with Optical Superresolution Methods : From the Test Tube to Models of Disease. *Neurophotonics* **2016**, *3*, 041807.

(15) Ye, R.; Liu, Y.; Zhang, H.; Su, H.; Zhang, Y.; Xu, L.; Hu, R.; Kwok, R. T. K.; Wong, K. S.; Lam, J. W. Y.; et al. Non-Conventional Fluorescent Biogenic and Synthetic Polymers without Aromatic Rings. *Polym. Chem.* **2017**, *8*, 1722−1727.

(16) Shimanovich, U.; Pinotsi, D.; Shimanovich, K.; Yu, N.; Bolisetty, S.; Adamcik, J.; Mezzenga, R.; Charmet, J.; Vollrath, F.; Gazit, E.; et al. Biophotonics of Native Silk Fibrils. *Macromol. Biosci.* **2018**, *18*, 1700295.

(17) Diaferia, C.; Sibillano, T.; Balasco, N.; Giannini, C.; Roviello, V.; Vitagliano, L.; Morelli, G.; Accardo, A. Hierarchical Analysis of Self-Assembled PEGylated Hexaphenylalanine Photoluminescent Nanostructures. *Chem. - Eur. J.* **2016**, *22*, 16586−16597.

(18) Diaferia, C.; Sibillano, T.; Altamura, D.; Roviello, V.; Vitagliano, L.; Giannini, C.; Morelli, G.; Accardo, A. Structural Characterization of PEGylated Hexaphenylalanine Nanostructures Exhibiting Green Photoluminescence Emission. *Chem. - Eur. J.* **2017**, *23*, 14039−14048.

(19) Pinotsi, D.; Grisanti, L.; Mahou, P.; Gebauer, R.; Kaminski, C. F.; Hassanali, A.; Kaminski Schierle, G. S. Proton Transfer and Structure-Specific Fluorescence in Hydrogen Bond-Rich Protein Structures. *J. Am. Chem. Soc.* **2016**, *138*, 3046−3057.

(20) Joseph, S. K.; Kuritz, N.; Yahel, E.; Lapshina, N.; Rosenman, G.; Natan, A. Proton-Transfer-Induced Fluorescence in Self-Assembled Short Peptides. *J. Phys. Chem. A* **2019**, *123*, 1758.

(21) Wolfbeis, O. S. An Overview of Nanoparticles Commonly Used in Fluorescent Bioimaging. *Chem. Soc. Rev.* **2015**, *44*, 4743−4768.

(22) Alfano, R.; Pu, Y. Optical Biopsy for Cancer Detection. *Lasers for Medical Applications* **2013**, 325.

(23) Deisseroth, K. Optogenetics. *Nat. Methods* **2011**, *8*, 26−29.

(24) Amdursky, N.; Molotskii, M.; Gazit, E.; Rosenman, G. Elementary Building Blocks of Self-Assembled Peptide Nanotubes. *J. Am. Chem. Soc.* **2010**, *132*, 15632−15636.

(25) Hauser, C. A. E.; Zhang, S. Peptides as Biological Semiconductors. *Nature* **2010**, *468*, 516−517.

(26) Weston, K. D.; Carson, P. J.; Metiu, H.; Buratto, S. K. Room-Temperature Fluorescence Characteristics of Single Dye Molecules Adsorbed on a Glass Surface. *J. Chem. Phys.* **1998**, *109*, 7474−7485.

(27) Ghosh, S.; Chizhik, A. M.; Karedla, N.; Dekaliuk, M. O.; Gregor, I.; Schuhmann, H.; Seibt, M.; Bodensiek, K.; Schaap, I. A. T.; Schulz, O.; et al. Photoluminescence of Carbon Nanodots : Dipole Emission Centers and Electron−Phonon Coupling. *Nano Lett.* **2014**, *14*, 5656−5661.

(28) Empedocles, B. S. A.; Neuhauser, R.; Shimizu, K.; Bawendi, M. G. Photoluminescence from Single Semiconductor Nanostructures. *Adv. Mater.* **1999**, *11*, 1243−1256.

(29) Moerner, W. E.; Fromm, D. P. Methods of Single-Molecule Fluorescence Spectroscopy and Microscopy. *Rev. Sci. Instrum.* **2003**, *74*, 3597−3619.

(30) Resch-Genger, U.; Grabolle, M.; Cavaliere-Jaricot, S.; Nitschke, R.; Nann, T. Quantum Dots versus Organic Dyes as Fluorescent Labels. *Nat. Methods* **2008**, *5*, 763−775.

(31) Basche, T. Fluorescence Intensity Fluctuations of Single Atoms, Molecules and Nanoparticles. *J. Lumin.* **1998**, *76-77*, 263−269.

(32) Nirmal, M.; Dabbousi, B. O.; Bawendi, M. G.; Macklin, J. J.; Trautman, J. K.; Harris, T. D.; Brus, L. E. Fluorescence Intermittency in Single Cadmium Selenide Nanocrystals. *Nature* **1996**, *383*, 802−804.

(33) Efros, A. L.; Nesbitt, D. J. Origin and Control of Blinking in Quantum Dots. *Nat. Nanotechnol.* **2016**, *11*, 661−671.

(34) Yuan, G.; Gómez, D. E.; Kirkwood, N.; Boldt, K.; Mulvaney, P. Two Mechanisms Determine Quantum Dot Blinking. *ACS Nano* **2018**, *12*, 3397−3405.

(35) Khan, S.; Li, W.; Karedla, N.; Thiart, J.; Gregor, I.; Chizhik, A. M.; Enderlein, J.; Nandi, C. K.; Chizhik, A. I. Charge-Driven Fluorescence Blinking in Carbon Nanodots. *J. Phys. Chem. Lett.* **2017**, *8*, 5751−5757.

(36) Chizhik, A. M.; Stein, S.; Dekaliuk, M. O.; Battle, C.; Li, W.; Huss, A.; Platen, M.; Schaap, I. A. T.; Gregor, I.; Demchenko, A. P.; et al. Super-Resolution Optical Fluctuation Bio-Imaging with Dual-Color Carbon Nanodots. *Nano Lett.* **2016**, *16*, 237−242.

(37) Bagshaw, C. R.; Cherny, D. Blinking Fluorophores: What Do They Tell Us about Protein Dynamics? *Biochem. Soc. Trans.* **2006**, *34*, 979−982.

DOI: 10.1021/acsphotonics.9b00685
ACS Photonics XXXX, XXX, XXX−XXX

(38) Rust, M. J.; Bates, M.; Zhuang, X. Sub-Diffraction-Limit Imaging by Stochastic Optical Reconstruction Microscopy (STORM). *Nat. Methods* **2006**, *3*, 793−795.

DOI: 10.1021/acsphotonics.9b00685
ACS Photonics XXXX, XXX, XXX−XXX